The Open Access Journal of Science and Technology
vol. 5 (2017), Article ID 101242, 15 pages
doi:10.11131/2017/101242

AgiAl Publishing House
http://www.agialpress.com/

Research Article

Mechanism of Randall's Plugs Development

Felix Grases[1], Otakar Söhnel[2], Antonia Costa-Bauza[1], and Tomáš Loučka[2]

[1] *Laboratory of Renal Lithiasis Research, University Institute of Health Sciences Research (IUNICS-IdISPa), University of Balearic Islands, Palma of Mallorca, Spain*
[2] *University of J.E. Purkyně, Faculty of Environmental Studies, Ústí n.L., Czech Republic*

Abstract. Mechanism of formation and development of intraluminal concretion, also called Randall's plug, extracted from a female patient forming calcium oxalate dihydrate (COD) calculi was examined. Some of these calculi were connected to the papillary tip, and had connections with the interior of the papilla with finger-like extensions in the collecting duct (CD). The intraluminal concretion consisted of inter-grown COD crystals of irregular size (30–100 μm), approximately 5% of biological hydroxyapatite (BHAP) and an organic matter. Urine of the patient was moderately supersaturated with respect to COD and amorphous calcium phosphate (ACP). Model of kidney, recently refined by Robertson, was used in calculations. Calculated Reynolds number indicated that the flow of liquid through tubules was purely laminar with parabolic velocity profile. COD crystals formed at the beginning of ascending loop of Henle by heterogeneous nucleation. Concentration of COD crystals in urine was limited and considered equal to concentration of crystals during crystaluria. The free particle and the fixed particle mechanisms were considered. The free particle mechanism assumes formation of a single crystal or agglomerate of crystals blocking the CD by virtue of size. The growth of COD crystals at concrete urinary supersaturation was too slow for a single crystal to attain size with settling velocity faster than the translation flow rate of liquid. Hydrodynamic shear caused aggregation of COD solid particles dispersed in a liquid flowing in the nephron. Number of COD crystals present in urine was not sufficient for formation of fractal agglomerate blocking the Bellini duct. Similarly, a fractal agglomerate of urinary phosphate present in the form of Posner's clusters was not large enough to obstruct the Bellini duct. The opening of the CD could not be obstructed by a single crystal of COD or fractal agglomerate composed of either COD crystals or calcium phosphate clusters, formed in urine by virtue of size. Solid objects not immobilised inside the CD were always washed out by urine flow from the CD of any orientation (also upward-draining CD). The formation and development of plug of our patient was explained by the fixed particle mechanism assuming that Randall's plug developes from crystal(s) attached directly to the tubule wall. The plug was modelled as concretion composed of successive layers of COD crystals originating on the top of underlying layer. When growth of a layer stopped, its surface was covered by organic matter that served as a substrate for nucleation of a new layer. The time of plug development was estimated as the time a COD crystal needed to reach the opposite side of the duct plus duration of interruptions of crystalline growth when plug surface was covered by a layer of organic matter and phosphatic particles were incorporated into concretion. The flux of Posner's clusters arriving to the concretion surface was estimated from theory of Brownian motion. These calculations suggested that obstruction of the Bellini duct of our patient by the Randall's plug occurred over a period of approximately 4 months after nucleus of concretion became attached to the duct wall or on the papillary tip.

Keywords: Nephrocalcinosis, Randall's plugs, calcium oxalate dihydrate, biological hydroxyapatite, Posner's clusters.

Corresponding Author
Felix Grases
fgrases@uib.es

Editor
Vincenzo Bramanti

Dates
Received 1 July 2016
Accepted 10 April 2017

1. Introduction

Clinicians commonly observe renal papillary calcifications during endoscopic intrarenal surgery for removal of renal stones. These calcifications can be classified as two clearly different entities [1]. One type results from a subepithelial calcification (hydroxyapatite) of the renal papilla following pre-existing injury. The disruption of the papillary epithelial layer by biological hydroxyapatite (BHAP) plaque becomes the nidus of a calcium oxalate (CaOx) papillary calculus, known as Randall's plaque [2–8]. These intrapapillary calcifications initiate in the thin-loop basement membranes, in basement membranes of collecting tubules, and in the vasa recta [4–7]. These are all collagen rich regions [9], and the presence of carboxylate groups alters the collagen so it acts as heterogeneous nucleant of BHAP [10].

The other type of calcification is intraluminal crystalline deposits along the inner medullary collecting ducts (CD) and the ducts of Bellini, known as Randall's plugs. These deposits occasionally protrude from dilated openings of the ducts of Bellini and sometimes exhibit crystalline material growing from their distal ends. The amount and size of the intraluminal deposits vary with type of stones formed by patient. The tubular plugs are composed of apatite and CaOx, exceptionally of cystine or sodium and ammonium acid urate, and organic matter [11, 12]. The Randall's plugs occur in the terminal CDs of patients with elevated pH, elevated calcium and oxalate concentrations and low citrate excretion [13].

Mechanism of Randall's plugs formation is still under discussion. In essence, interluminal deposits can be formed by the free or the fixed particle mechanism. The free particle mechanism assumes that during the residence time of urine in the CD an object that can obstruct the opening into the calyx develops by growth and/or agglomeration of smaller particles. The fixed particle mechanism postulates that crystals initially attached directly to tubule wall develop by crystal growth and agglomeration into an object obstructing the Bellini duct [14]. Authors of this concept using probabilistic approach arrived to a conclusion that vast majority of concretions form in the kidney by the fixed particle mechanism and the free particle mechanism can be active only at very rare and specific cases. This conclusion was recently contested by Robertson based on the updated computer model of kidney NEPHROSIM [15, 16]. The mathematical model of urine flow and changes in concentration of tubular liquid along the nephron suggested that CaOx crystals may become sufficiently large to become trapped in the CD and develop into Randall's plug.

We have reported a case of a female patient forming calcium oxalate dihydrate (COD) calculi [17]. Some of these calculi were connected to the papillary tip, and had connections with the interior of the papilla with finger-like extensions in the CD. Several of these extensions were extracted and their structure and composition studied using electron scanning microscope equipped with X-ray energy spectrometer. Performed studies, however, did not reveal mechanism of their formation.

In the present paper we discuss the possible mechanisms underlying the formation and development of these Randall's plugs.

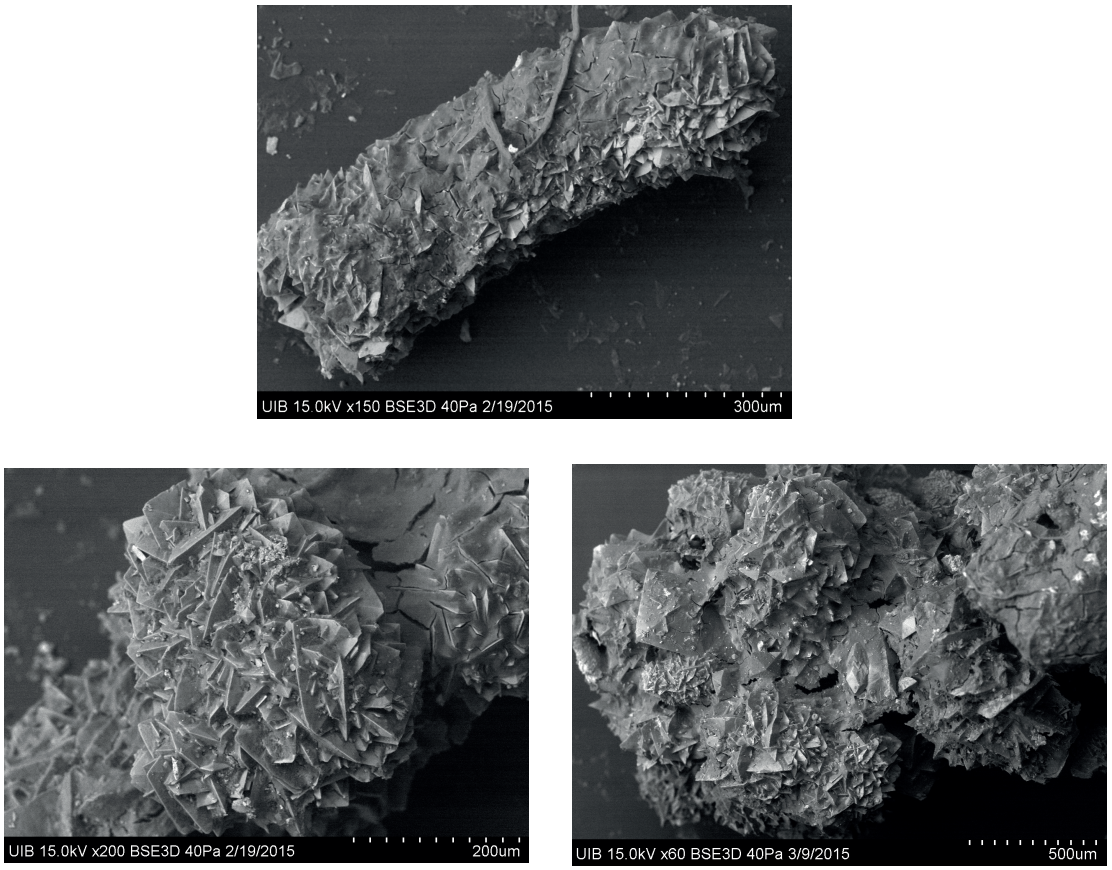

Figure 1: Scanning electron microscopy image of a plug blocking a Bellini duct of our patient and details of other plugs.

2. Method and Results

2.1. Randall's plug

The plugs of diameter about 2×10^{-4} m consisted of inter-grown COD crystals of irregular size (30–100 μm), approximately 5% of BHAP and an organic matter, Figure 1. Some large COD crystals were also observed. The distribution of phosphorus in the plugs was mostly uniform, although a few isolated regions had higher concentrations.

2.2. Urine

Urine is a variable non-steady state system the composition of which constantly changes and therefore conditions prevailing during formation and development of Randall's plug are difficult to specify precisely. Urine composition of the respective Randall's plug former shown in Table 1 was used for further considerations. The concentration of magnesium was not experimentally determined and was taken from literature [18]. This composition corresponded to typical urinary composition of patients with Randall's plugs [11].

The concentrations and activities of ionic species in urine of our patient at 37°C were computed using the programme MINTEQA2 [19] as $[Ca^{2+}] = 3.83 \times 10^{-3}$ mol L^{-1}, $[C_2O_4{}^{2-}] =$

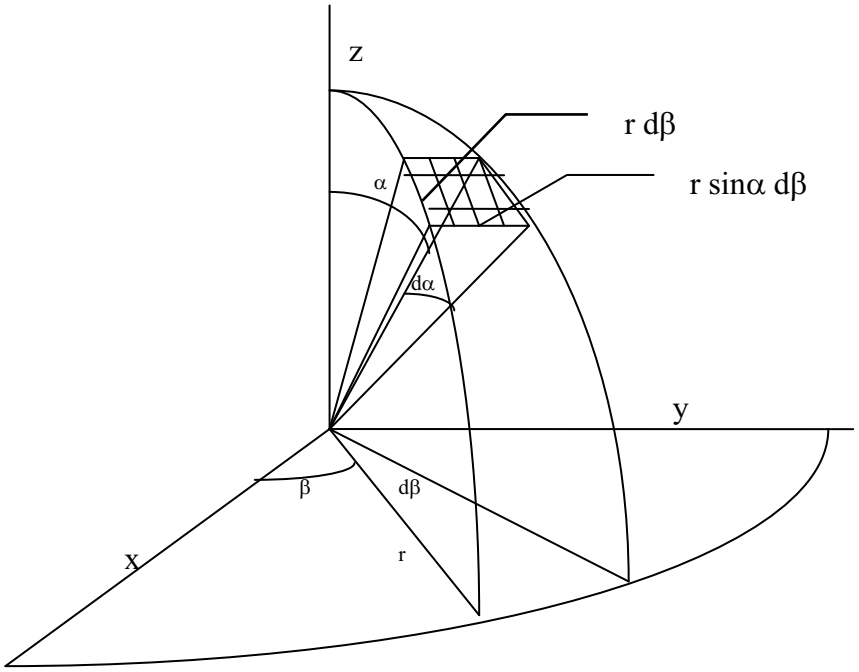

Figure 2: Spherical sector ($\alpha + d\alpha, \beta + d\beta$).

Table 1: Urine composition.

	Concentrations (mol m^{-3})	Ref
Ca(total)	9.98	[17]
Mg^{2+}	1.9	[18]
P(inorganic)	32.29	[17]
Oxalate	0.34	[17]
pH	6.8	[17]

Diuresis V_D = 1.5 L/24 h

1.14×10^{-4} mol L^{-1}, $[PO_4{}^{3-}] = 8.82 \times 10^{-8}$ mol L^{-1} and $a(Ca^{2+}) = 1.85 \times 10^{-3}$ mol L^{-1}, $a(C_2O_4{}^{2-}) = 5.49 \times 10^{-5}$ mol L^{-1} and $a(PO_4{}^{3-}) = 1.71 \times 10^{-8}$ mol L^{-1}. Supersaturation of this urine with respect to COD is

$$S = \left\{K_{a,ip}/K_{a,sp}\right\}^{1/2} = \left\{a\left(Ca^{2+}\right) a\left(C_2O_4{}^{2-}\right)/6.76 \times 10^{-9}\right\}^{1/2} = 3.87$$

where the thermodynamic solubility product $K_{a,sp}$ of COD is taken from [20]. This value of supersaturation is higher than the real value since ion pairing of Ca and oxalate with Na, K, Cl, SO_4 and citrate was not considered as contents of these elements were not determined in our patient urine. On the other hand, composition of urine fluctuates due to intermittent food and liquid ingestion. With changing urine composition varies its supersaturation. The supersaturation of urine fluctuates also during the Randall's plug formation and development. Thus the actual supersaturation oscillates and because it is impossible to quantify extent of these fluctuations the value calculated from the analytically determined composition of patient's urine is taken as an average value of supersaturation prevailing during plug formation.

The dynamic viscosity of urine is $\eta = \upsilon \times \rho_l = 0.841 \times 10^{-3}$ kg m^{-1} s^{-1}, where $\upsilon = 0.829 \times 10^{-6}$ m^2 s^{-1} is the kinematic viscosity [21] and $\rho_l = 1015$ kg m^{-3} is the density of urine [22].

2.3. Kidney

1.31×10^6 nephrons terminate in 320 CDs in a kidney according to Robertson model of kidney [15]. The nephron consists of proximal tubule, descending and ascending loop of Henle and distal tubule. Liquid in the nephron is approximately 10 times diluted compared to urine at the opening of the CD. Reabsorption of ionic species and water from filtrate entering the nephron from glomerulus proceeds during liquid transit through the nephron to the CD where water content is finally adjusted. The highest supersaturation of urine is reached at the opening of CD on the papilla. The average translation rate of liquid and the average transit time through the ascending loop of Henle are 1.8×10^{-4} m s^{-1} and 65 s and through the distal tubule 1.9×10^{-4} m s^{-1} and 31 s [15].

Diameter of the CD used in calculations corresponds to the plug size and therefore differs from Robertson model. The CD is a circular truncated cone with length $L_b = 2.7 \times 10^{-2}$ m and a radius $r_1 = 0.5 \times 10^{-4}$ m at the beginning and a radius $r_2 = 1 \times 10^{-4}$ m at the termination (opening) on the papilla. The volume of single CD is

$$V_B = (\pi/3)L_b \left[r_2^2 + r_2 r_1 + r_1^2\right] = 4.94 \times 10^{-10} \text{ m}^3$$

Assuming 1.5 L as an average diuresis (for 2 kidneys) and constant liquid throughput, the volume of liquid passing through single CD per second, i.e. the average volumetric flow rate of urine through Bellini duct is

$$Q = 1.5 \times 10^{-3}/[(2 \times 24 \times 3600) \times 320] = 2.71 \times 10^{-11} \text{ m}^3\text{s}^{-1}$$

The average translation flow rate of urine in the CD is (see Appendix I)

$$u = Q/\text{Ave}\left(\pi r^2\right) = 1.48 \times 10^{-3} \text{ ms}^{-1}$$

The flow of urine in the CD is fully laminar because the Reynolds number for flow in the circular duct is $\text{Re} = 2\, r_2\, Q / \upsilon\, \pi\, r_2^2 = 0.208$ (flow is fully laminar for $\text{Re} < 1$). The mean residence time of liquid in a CD (transit time) is

$$t_{av} = V_B/Q = 18.2 \text{ s}$$

3. Mechanisms of Randall's Plug Development

3.1. Free particle mechanism

The potential obstruction of the CD by a crystal or an agglomerate of COD and calcium phosphate crystals that are formed in urine will be examined. The free particle mechanism assumes that during the mean residence time of urine in the nephron and the CD a spherical object that can obstruct the opening into the calyx by virtue of size develops by growth of a single particle or by agglomeration of smaller particles [14].

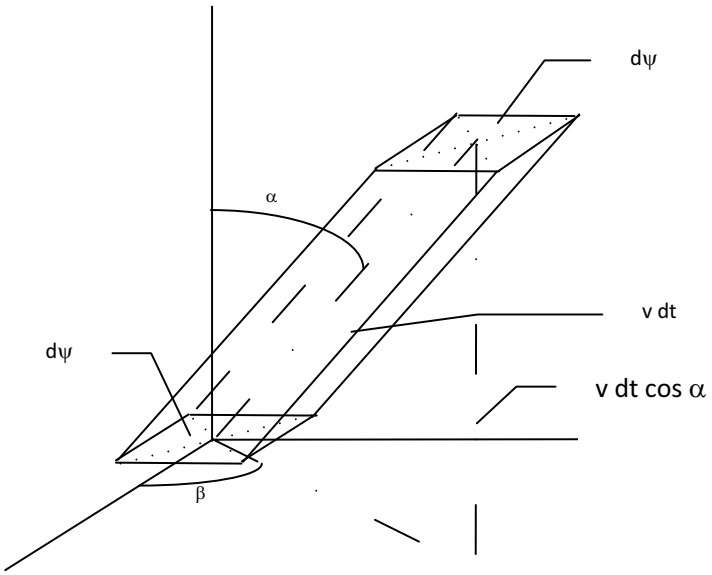

Figure 3: Oblique quadrangular prism.

3.1.1. Calcium oxalate dihydrate

COD crystals, molecular weight 0.164 kg mol^{-1}, density 2020 kg m^{-3} [23] occur in human urinary calculi as tetragonal bipyramids [24]. COD crystals form in supersaturated solutions by homogeneous or heterogeneous nucleation. The rate of homogeneous nucleation is given by [25]

$$J = \left(2D/d^5\right) \exp\left\{-k_v\sigma^3 v^2/\left[(k\,T)^3(\nu \ln S)^2\right]\right\}\ m^{-3}\ s^{-1} \quad (1)$$

where D is the ionic diffusion coefficient ($D = kT/(6\pi\eta r) = 1.46 \times 10^{-9}$ m^2 s^{-1}), d is the building unit diameter (4.1×10^{-10} m), k_v is 32 for a cube, σ is the interfacial tension (0.123 J m^{-2} [26]), ν is the number of ions in a molecule and v is the volume of the building unit ($v = M_w/\rho_s \nu\, N_A = 0.164 / \{2020 \times 2 \times 6.022 \times 10^{23}\} = 6.7 \times 10^{-29}$ m^3) and k is the Boltzmann's constant $k = 1.38 \times 10^{-23}$ kg m^2 s^{-2} K^{-1}. Substituting these values into eq. (1) describing the nucleation rate of COD gives

$$J = 4.27 \times 10^{38} \times \exp(-515) \sim 0\ m^{-3}s^{-1}$$

The rate of homogeneous nucleation at actual supersaturation was virtually zero. The onset of homogeneous nucleation of COD crystals, tentatively defined as formation of one nucleus per second in 1 m^3, i.e. the rate of nucleation J = 1 m^{-3} s^{-1}, occurs according to eq. (1) at S = 34.3. The actual urinary supersaturation of our patient - 3.87 - was much too low for homogeneous nucleation to be active and therefore COD crystals in urine originated on the foreign substrates present in urine by heterogeneous nucleation. Hence the number concentration of COD crystals in urine was limited and was approximately equal to concentration of crystals during crystaluria, 2.4×10^{10} m^{-3} [27].

Further considerations require the growth rate of COD crystal expressed as the rate of its radius increase in the form $dr/dt = k_g(S - 1)^n$, where k_g is the growth rate constant and n is an exponent. The growth rate in the COD-seeded system was 22 per cent of that for a COM-seeded system at the same supersaturation, for equivalent surface areas [28]. According to [29] k_g of

COD-seeded growth was 42 per cent lower than for COM and n = 2. Since k_g in the case of COM is 5.6×10^{-11} m s^{-1} [30], k_g for COD is in the range $(1.23 - 2.35) \times 10^{-11}$ m s^{-1}. The rate of growth of COD crystal is expressed by

$$dr/dt = (1.23 - 2.35) \times 10^{-11}(S - 1)^2 \text{ m s}^{-1} \quad (2)$$

The maximum size of crystals in the CD that originated in the ascending loop of Henle can be estimated as follows: Initial size of heterogeneous nucleus is supposed to be $r^* = 0.1 \times 10^{-6}$ m [16]. The residence time of a crystal nucleated at the beginning of the ascending loop of Henle and travelling in close vicinity of the tubular wall is 25 min [16]. Hence the maximum size of COD crystal achievable in the nephron is

$$r_{max} = r^* + (dr/dt) \times t = 0.1 \times 10^{-6} + (1.23\text{–}2.35) \times 10^{-11} \times 2.87^2 \times 25 \times 60 = (0.25\text{–}0.48) \times 10^{-6} \text{ m}$$

The maximum achievable radius of COD crystal, $(0.25 - 0.48) \times 10^{-6}$ m, was calculated under assumption that supersaturation of liquid in the nephron is the same as supersaturation at the opening of CD. According to Robertson model [16] the supersaturation of urine in the nephron is considerably lower than in the CD and thus the calculated maximum size of COD crystal is overestimated.

Any individual COD crystal cannot become large enough ($r \geq 0.5 \times 10^{-4}$ m) to obstruct the CD during its residence time in the nephron as a result of size.

The parabolic velocity profile of laminar flow of liquid in a tubule is described by

$$u(R) = 2u_{av}\left[1 - (R/r)^2\right] \quad (3)$$

where r is the radius of the tubule and R is the distance from the tubule axis. The flow pattern can be considered as a set of thin concentric shells of fluid sliding over one another. The velocity of the fluid at the centre line is twice the average velocity of the fluid, u_{av}, and zero at the first shell adjoining tubular wall. A crystal close to the tubule wall travels in a shell moving with considerably lower velocity than the average translation flow rate. A liquid in a shell adjacent to the CD wall with thickness of 0.50×10^{-6} and 0.96×10^{-6} m moves according to eq. (3) with the average velocity 1.48×10^{-5} m s^{-1} and 2.77×10^{-5} m s^{-1}, respectively.

Settling velocity of a spherical particle in the laminar flow of liquid is

$$w = 2(\rho_s - \rho_l)gr^2/9\eta \quad (4)$$

r is the radius of spherical particle and g is the acceleration due to gravity 9.81 m s^{-2}. Settling velocity calculated from eq. (3) of COD crystal with radius 0.25×10^{-6} m and 0.48×10^{-6} m is 1.6×10^{-7} m s^{-1} and 5.7×10^{-7} m s^{-1}, respectively. This velocity is by about four orders of magnitude smaller than the average translation flow rate of liquid in the Bellini duct. Even liquid close to tubular wall moves about two orders of magnitude faster than the settling velocity of largest COD crystal which can occur in the CD.

Therefore any single COD crystal formed and developed in the nephron and the CD cannot be retained in the CD by virtue of its size and is invariably washed out from the CD of any orientation, even upward-draining duct, by flow of urine.

Solid particles of COD dispersed in urine flowing through the CD are exposed to hydrodynamic shear that causes their aggregation by orthokinetic mechanism [31]. Further a case that

an object blocking the opening of the CD formed by agglomeration of COD crystals will be examined.

A spherical agglomerate of COD crystals with radius 1.0×10^{-4} m can block the opening of the CD. This agglomerate composed of crystals with radius 0.48×10^{-6} m with packing density $\xi = 0.07$ (Appendix II) consists of $4.19 \times 1.0 \times 10^{-12} \times 2020 \times 0.07/0.164 = 3.61 \times 10^{-9}$ mol of COD. Total amount of calcium oxalate over equilibrium contained in 1 litre of urine is

$$1.14 \times 10^{-4} - \left[6.78 \times 10^{-9} / \left(0.48^2 \times 3.83 \times 10^{-3}\right)\right] = 1.06 \times 10^{-4} \text{ mol L}^{-1}$$

where 0.48 is the activity coefficient of divalent ion. Let assume an unrealistic case that all calcium oxalate over equilibrium contained is present as crystals that form agglomerate. Volume of liquid in which agglomeration proceeds before formed object reaches the opening of CD is equal to the average transit time of urine through the nephrons from the point of crystals origination (beginning of ascending loop of Henle) to the CD opening multiplied by the average volumetric flow rate at the Bellini duct, i.e. $(65 + 31 + 18) \times 2.71 \times 10^{-11} = 3.09 \times 10^{-9}$ m^3. The molar mass of COD in excess of equilibrium available in this volume of urine is $3.09 \times 10^{-9} \times 1.06 \times 10^{-4} \times 10^3 = 3.3 \times 10^{-10}$ mol. This mass hypothetically available for forming an agglomerate of COD crystals is about one order of magnitude smaller than the molar mass of the agglomerate that can block the opening of the CD. Furthermore, the number of crystals with size 0.48×10^{-6} m forming the blocking agglomerate

$$3.61 \times 10^{-9} / \left[4.19 \times \left(0.48 \times 10^{-6}\right)^3 \times 2020/0.164\right] = 6.32 \times 10^5$$

is contained in $6.32 \times 10^5/2.4 \times 10^{10} = 2.63 \times 10^{-5}$ m^3 of urine. This volume of urine passes the Bellini duct in $2.63 \times 10^{-5}/2.71 \times 10^{-11} = 9.7 \times 10^5$ s, i.e. 269 days.

Molar mass and number of crystals of COD hypothetically available for formation of agglomerate clearly demonstrate that size of this agglomerate is not sufficiently large to block the Bellini duct.

3.1.2. Calcium phosphate

The urine of our patient was supersaturated with respect to amorphous calcium phosphate (ACP) with the thermodynamic solubility product $K_{a,sp} = 6.31 \times 10^{-25}$ mol^5 L^{-5} [32], which is the initial phase that precipitates from solution

$$S = \left\{\left[a\left(Ca^{2+}\right)\right]^3 \left[a\left({PO_4}^{3-}\right)\right]^2 / 6.31 \times 10^{-25}\right\}^{1/5} = 1.24$$

A fraction of the solute in phosphate solutions is present in the form of Posner's clusters [33–35]. Roughly 50% of phosphate is bound in the Posner's clusters at high supersaturation [33]. Let assume the same fraction of phosphate in urine bound in these clusters with a diameter 1×10^{-9} m, i.e. volume 5.23×10^{-28} m^3, and a presumed formula $Ca_9(PO_4)_6$ though urine is only slightly supersaturated with respect of ACP [36].

Let consider the case that all Posner's clusters present in a volume of urine produced by a single CD multiplied by the average transit time of liquid through the nephron forms an agglomerate. The number of clusters present in urine is $N = [{PO_4}^{3-}] \times 10^3 \times N_A \times 0.5/6 =$

4.43×10^{18} m^{-3}. The average transit time of urine through the nephron from the point of crystals origination (beginning of ascending loop of Henle) and the CD is 114 s. The number of clusters present in this volume of urine is $N_c = 4.43\times10^{18}\times114\times Q = 1.37\times10^{10}$. Radius of a single loosely packed spherical agglomerate (packing density $\xi = 5\times10^{-3}$) composed of all these clusters is $r = (N_c\times5.23\times10^{-28}/4.19\times5\times10^{-3})^{1/3} = 7\times10^{-6}$ m. This radius is considerably smaller than radius of the Bellini duct and therefore the opening of the CD cannot be obstructed by a phosphatic agglomerate.

The opening of the CD cannot be obstructed by a single crystal of COD or an agglomerate composed of either COD crystals or calcium phosphate clusters, formed in urine by virtue of size. Therefore intraluminal concretion of our patient was not formed by the free particle mechanism and was formed by a different mechanism.

3.2. Fixed particle mechanism

The fixed particle mechanism assumes that Randall's plug develops from crystal(s) attached directly to the tubule wall. Next, the potential obstruction of the CD by a concretion originated on a crystalline substrate immobilized on the tubular wall will be examined.

COD crystallizes from solutions as tetragonal bipyramidal crystals [24]. The time for a single crystal attached to a CD wall and growing in urine with supersaturation S = 3.87 to reach the size 2×10^{-4} m (plug diameter) is

$$t \sim 2\times10^{-4}/(1.23-2.35)\times10^{-11}\times2.87^2 = (1.03-1.97)\times10^6 \text{ s} \sim 12-23 \text{ days}$$

The plug extracted from a CD was modeled as a concretion composed of successive layers of COD crystals originating on the top of underlying layer. When growth of a layer stops, its surface is covered by organic matter that serves as a nucleation substrate for a new layer. Thus the time needed for duct blockage by COD crystals can be estimated as the sum of the time a COD crystal needs to reach the opposite side of the duct and the sum of intervals of interruption of plug growth (the induction periods of new crystal layers formation by surface nucleation on the organic substrate) when crystalline surface of plug is covered by a layer of organic matter.

The time during which the growth of crystalline concretion is interrupted (the sum of induction period new layers nucleation) can be estimated from the amount of phosphorus in the plug.

Calcium phosphate is not isomorphous with COD and hence cannot be incorporated directly into oxalate crystals. Therefore phosphatic particles, nano-sized Posner's clusters, can be incorporated only into amorphous organic matter that periodically covers crystalline part of the plug. ACP clusters arriving to the layer of organic matter covering the concretion, attach to its surface, densify and become an integral part of the concretion and gradually transform to BHAP [34].

The flux of Posner's clusters arriving to the concretion surface can be estimated as follows. An elementary volume of urine with the average translation rate 1.48×10^{-3} m s^{-1} remains in contact with a square area $A_n = 1\times10^{-12}$ m^2 of a COD concretion surface oriented toward the opposite wall of the CD (along the x-axis) for

$$t_c = 1\times10^{-6}/1.48\times10^{-3} = 6.76\times10^{-4} \text{ s}$$

The Posner's clusters are so small that they perform Brownian motion. The mean (arithmetic) particle displacement of a particle with radius r_c along the x-axis due to Brownian motion over a time interval t_c is [37]

$$\Delta\lambda = (k\,T/3\pi\eta r_c)^{1/2} t_c^{1/2} = 8.47 \times 10^{-7}\ m$$

The number of clusters present in 1 m^3 of urine, N_c, assuming that 50% of phosphate ions are bound in the Posner's clusters is $4.42 \times 10^{18}\ m^{-3}$ (see above). The number of Posner's clusters that arrives at the surface area A_n per second is (Appendix III)

$$N(\varepsilon) = \frac{1}{4} N_c A_n \Delta\lambda / t_c = 1.38 \times 10^3\ s^{-1}$$

and have volume $V = 7.25 \times 10^{-25} m^3$. Assuming that every cluster arriving to the surface A_n of the concretion is captured, 2.23×10^{-21} kg of BHAP (density 3080 kg m^{-3} [23]) per second is incorporated into the concretion.

Mass of a section of concretion with surface area $1 \times 10^{-12}\ m^2$ and length 2×10^{-4} m is 4.04×10^{-13} kg. Since the plug contains 5 wt.% of calcium phosphate, this section contains 2.02×10^{-14} kg of BAHP. Incorporation of this mass of calcium phosphate into concretion takes

$$2.02 \times 10^{-14} / 2.23 \times 10^{-21} = 9.06 \times 10^6\ s,\ \text{i.e. } 105\ \text{days}$$

Therefore the time during which this concretion developed is the sum of the growth period of COD crystal and the period of calcium phosphate clusters incorporation, i.e. (12 – 23) + 105 ~ 117 – 128 days, i.e. 3.9 – 4.3 months, under favourable conditions.

Contribution of the protein fraction to a plug volume was not considered because of the absence of any relevant model. Therefore the time of concretion development may be slightly different from the calculated value.

4. Discussion

Mechanism of formation and development of intraluminal concretion extracted from the CD of a female patient was examined. The computer kidney model NEPHROSIM demonstrates that supersaturation of urine with respect to COD increases from glomerulus and peaks at the beginning of the ascending loop of Henle, then decreases due to reabsorption of ions in loop of Henle and proximal tubule and increases again in the CD due to reabsorption of water. The highest level of urinary supersaturation is at the opening of the Bellini duct [15, 16] and this value was used in calculations.

The size of crystals at the Bellini duct was calculated using the longest period of growth (crystals travelled close to the tubule wall) and the highest supersaturation (reached only in the Bellini duct). This was a maximum achievable size of an individual crystal in the opening of the CD. Settling velocity of this crystal was considerably slower than the translation flow rate of urine in the CD. Hence, all individual crystals developed in the nephron are always washed out from the CD of any orientation and cannot serve as a centre for gradual development of a blocking intraluminal concretion.

Hydrodynamic shear acting on solid particles, nucleated at the beginning of ascending loop of Henle, during their progress through the nephron causes their aggregation into larger objects by

mechanism of orthokinetic agglomeration. Calculations showed that the agglomerate blocking the Bellini duct is composed of substantially larger amount of mass and number of individual particles of COD or ACP than quantity available in the volume of liquid passing single CD during the average transit time of urine through the nephron and the CD. In fact, the difference between amount of material, both mass and number of crystals, required for formation of the blocking object and actually available material is rather vast.

Although in our calculations the most favourable conditions for the free particle mechanism, such as the longest transit time, the highest supersaturation, agglomeration of all particles present in a given volume, were considered, maximum attainable size of crystalline particle (single crystal or agglomerate) was not sufficiently large for being retained in the Bellini duct of any orientation by virtue of size. Thus the Randall's plug extracted from of our patient was not formed by gradual development of unattached particle, be it single crystal or agglomerate, retained in the CD into a concretion blocking its opening, i.e. by the free particle mechanism.

The studied Randall's plug developed from a crystalline particle (particles) firmly attached to the inner wall of the CD or papillary tip, i.e. by the fixed particle mechanism. Period of the plug development was roughly estimated from the phosphorus content of the concretion. Nano-sized Posner's clusters existing in urine perform Brownian motion and their flux to the surface of concretion can be evaluated from the theory of Brownian motion. Assuming that each cluster arriving to the surface was incorporated into the plug, the time needed for transport of 5 per cent of the plug mass indicated the total interval during which the concretion accumulated phosphorus. This period plus time during which the growing crystal would reach the opposite side of the CD indicated the time of the studied plug formation. The period of plug formation estimated in this way should be regarded with caution as a first rough approximation since several important factors, such as contribution of organic matter to plug volume, fluctuation of urine composition during plug development, influence of inhibitors of crystallization and promoters of agglomeration, which may considerably modify the kinetics of plug development, were not known and hence were not considered.

5. Conclusions

The calculations presented here indicate that a free particle mechanism cannot account for formation of the Randall's plug composed of COD, BHAP and organic matter that obstructed the Bellini's duct of our patient. This plug was formed by the fixed particle mechanism. Calculations suggest that plug obstructing the Bellini duct of our patient developed probably over a period of approximately 4 months.

List of symbols

a(X): the activity of ion X

A_n: surface (m^2)

Ave: average value

c(X): analytical (total) concentration of ion X (mol L^{-1})

D_m: the mass aggregate fractal dimension (-)

d: diameter (m)
g: acceleration due to gravity (m s^{-1})
J: nucleation rate (m^{-3} s^{-1})
$K_{a,sp}$: the thermodynamic solubility product (expressed in activities)
$K_{a,ip}$: the ionic activity product
k: the Bolzmann's constant (1.38×10^{-23} kg m^2 s^{-2} K^{-1})
k_v: volume shape factor (-)
L_b: length of the collecting duct (m)
M_w: molecular weight (kg/mol^{-1})
N_A: Avogadro's number (6.022×10^{23} mol^{-1})
N_c: number of clusters
$N(\varepsilon)$: number of clusters that arrives to the surface per second (s^{-1})
Q: volumetric flow rate (m^3 s^{-1})
r: radius (m)
$\Re$: dimensionless size (-)
S: supersaturation (-)
T: temperature (K)
t: time (s)
t_{av}: the mean residence time (s)
t_c: duration of contact of an elemental volume of urine with surface (s)
u: the translation flow rate of the liquid (m s^{-1})
u_{av}: the average translation flow rate (m s^{-1})
v: volume of building unit (m^3)
V: volume (m^3)
V_B: volume of the collecting duct (m^3)
w: settling velocity (m s^{-1})

Greek

$\Delta\lambda$: mean particle displacement (m)
η: dynamic viscosity (kg m^{-1} s^{-1})
ξ: packing density (-)
ν: number of ions constituting the building unit
υ: kinematic viscosity (m^2 s^{-1})
$\rho_{l,s}$: density of liquid and solid phase (kg m^{-3})
σ: interfacial tension (J m^{-2})

Abbreviations

ACP: amorphous calcium phosphate

BHAP: biological hydroxyapatite

CaOx: calcium oxalate

CD: collecting duct

COD: calcium oxalate dihydrate

Appendix I. Average of Function

Function *f(x)* can be integrated over an interval $\langle a, b\rangle$. Then the average of function *f(x)* in this interval is

$$\mathrm{Ave}(f(x)) = [(1/(b-a)] \times \int_a^b f(x)dx$$

Appendix II. Packing Density

Objects formed by agglomeration are governed by fractal geometry. Mass contained in a fractal agglomerate (a non-compact object containing internal voids) increases with its radius according to $m(r_a) \sim {r_a}^{Dm}$, where D_m represents the mass agglomerate fractal dimension. D_m is 2.5 for the three dimensional fractal agglomerate formed by the random motion of particles that irreversibly associate with a growing germ [38]. The more D_m deviates from 3, the higher degree of fractality object exerts.

Number of uniform particles N_a with radius r_o constituting a compact agglomerate (without internal voids) with radius r_a increases proportionally to the third power of its dimensionless size $\mathfrak{R} = r_a/r_o$, i.e. $N_a \sim \mathfrak{R}^3$. Number of uniform particles N_f constituting a fractal agglomerate is proportional to $\mathfrak{R}^{2.5}$.

The packing density ξ expresses the proportion of space filled by the particles, is

$$\xi = N_f/N_a = 1/\mathfrak{R}^{1/2}$$

Appendix III. Particles moving in a given direction

Clusters due to random Brownian motion move in all directions. If $N(\chi)$ clusters situated in the centre of sphere move from the centre with the same velocity then the velocity vectors fill volume of a sphere with radius r. Fraction of clusters, $N(\zeta)$, that moves in the direction of a narrow spherical sector, characterized in polar coordinates as $(\alpha + d\alpha, \beta + d\beta)$, see Figure 2, is

$$\begin{aligned} N(\zeta) &= N(\chi) \times \text{Volume of spherical sector / Volume of sphere} \\ &= N(\chi) \times (1/3) \times r^3 \times \sin\alpha \times d\alpha \times d\beta/(4\pi r^3/3) \end{aligned}$$

Clusters occurring in the oblique quadrangular prism with volume $V = v \times dt \times d\psi \times \cos\alpha$ and moving with velocity v in the right direction would reach in time dt a small plane with area $d\psi$ situated in the centre of sphere, see Figure 3. Number of these clusters is

$$N(\theta) = V \times N(\zeta) = N(\chi) \times v \times dt \times d\psi \times \cos\alpha \times \sin\alpha \times d\alpha \times d\beta/4\pi$$

Total number of clusters reaching plane $d\psi$ from the half space in time dt is

$$N(\varepsilon) = (N(\chi) \times dt \times d\psi/4\pi) \int_{\alpha=0}^{\alpha=\pi/2} \int_{\beta=0}^{\beta=2\pi} \cos\alpha \sin\alpha \, d\alpha \, d\beta = \frac{1}{4} \times N \times d\psi \times dt$$

Competing Interests

The authors declare no competing interests.

Ethical Approval

This article does not contain any studies with human participants or animals performed by any of the authors.

Acknowledgements

This work was supported by grant PI 14/00853 from the Ministerio de Economia y Competitividad (Gobierno de España), and by FEDER funds (European Union). CIBER Fisiopatología Obesidad y Nutrición (CB06/03), Instituto de Salud Carlos III, Spain, also provided support.

References

[1] S. R. Khan and B. K. Canales, "Unified theory on the pathogenesis of Randall's plaques and plugs," *Urolithiasis*, vol. 43, supplement 1, pp. 109–123, 2015.

[2] A. Randall, "The origin and growth of renal calculi," *Annals of Surgery*, vol. 105, no. 6, pp. 1009–1027, 1937.

[3] E. L. Prien, "The Riddle of Randall's Plaques," *The Journal of Urology*, vol. 114, no. 4, pp. 500–507, 1975.

[4] A. P. Evan, J. E. Lingeman, F. L. Coe et al., "Randall's plaque of patients with nephrolithiasis begins in basement membranes of thin loops of Henle," *The Journal of Clinical Investigation*, vol. 111, no. 5, pp. 607–616, 2003.

[5] S. C. Kim, F. L. Coe, W. W. Tinmouth et al., "Stone formation is proportional to papillary surface coverage by Randall's plaque," *The Journal of Urology*, vol. 173, no. 1, pp. 117–119, 2005.

[6] R. C. O'Connor, E. M. Worcester, A. P. Evan et al., "Nephrolithiasis and nephrocalcinosis in rats with small bowel resection," *Urological Research*, vol. 33, no. 2, pp. 105–115, 2005.

[7] A. P. Evan, F. L. Coe, S. R. Rittling et al., "Apatite plaque particles in inner medulla of kidneys of calcium oxalate stone formers: osteopontin localization," *Kidney International*, vol. 68, no. 1, pp. 145–154, 2005.

[8] F. Grases, A. Costa-Bauzá, C. R. Bonarriba, E. C. Pieras, R. A. Fernández, and A. Rodríguez, "On the origin of calcium oxalate monohydrate papillary renal stones," *Urolithiasis*, vol. 43, supplement 1, pp. 33–39, 2015.

[9] A. P. Evan, E. J. Weinman, X.-R. Wu, J. E. Lingeman, E. M. Worcester, and F. L. Coe, "Comparison of the pathology of interstitial plaque in human ICSF stone patients to NHERF-1 and THP-null mice," *Urological Research*, vol. 38, no. 6, pp. 439–452, 2010.

[10] A. Takeuchi, C. Ohtsuki, T. Miyazaki et al., "Heterogeneous nucleation of hydroxyapatite on protein: Structural effect of silk sericin," *Journal of the Royal Society Interface*, vol. 2, no. 4, pp. 373–378, 2005.

[11] S. R. Khan, B. Finlayson, and R. Hackett, "Renal papillary changes in patient with calcium oxalate lithiasis," *Urology*, vol. 23, no. 2, pp. 194–199, 1984.

[12] A. Evan, R. Unwin, and J. Williams, Jr., "Renal Stone Disease: A Commentary on the Nature and Significance of Randall's Plaque," *Nephron Physiology*, vol. 119, no. 4, pp. p49–p53, 2011.

[13] M. P. Linnes, A. E. Krambeck, L. Cornell et al., "Phenotypic characterization of kidney stone formers by endoscopic and histological quantification of intrarenal calcification," *Kidney International*, vol. 84, no. 4, pp. 818–825, 2013.

[14] B. Finlayson and F. Reid, "The expectation of free and fixed particles in urinary stone disease," *Investigative Urology*, vol. 15, no. 6, pp. 442–448, 1978.

[15] W. G. Robertson, "Kidney models of calcium oxalate stone formation," *Nephron - Physiology*, vol. 98, no. 2, pp. 21–30, 2004.

[16] W. G. Robertson, "Potential role of fluctuations in the composition of renal tubular fluid through the nephron in the initiation of Randall's plugs and calcium oxalate crystalluria in a computer model of renal function," *Urolithiasis*, vol. 43, no. 1, pp. 93–107, 2014.

[17] F. Grases, O. Söhnel, A. Costa-Bauza, A. Servera, and J. Benejam, "A Case of Randall's Plugs Associated to Calcium Oxalate Dihydrate Calculi," *Urology Case Reports*, vol. 7, pp. 37–38, 2016.

[18] W. Jahnen-Dechent and M. Ketteler, "Magnesium basics," *Clinical Kidney Journal*, vol. 5, supplement 1, pp. i3–i14, 2012.

[19] JD. Allison, DS. Brown, and KJ. Novo-Gradac, MINTEQA/PRODEFA2, A geochemical assessment model for environmental System: Version 3.0 User's Manual, U. S. Environmental Protection Agency 1991; EPA/6003-91/021.

[20] J. Streit, L.-C. Tran-Ho, and E. Königsberger, "Solubility of the three calcium oxalate hydrates in sodium chloride solutions and urine-like liquors," *Monatshefte für Chemie*, vol. 129, no. 12, pp. 1225–1236, 1998.

[21] B. A. Inman, W. Etienne, R. Rubin et al., "The impact of temperature and urinary constituents on urine viscosity and its relevance to bladder hyperthermia treatment," *International Journal of Hyperthermia*, vol. 29, no. 3, pp. 206–210, 2013.

[22] M. Lee, "Basic skills in interpreting laboratory data. Ch 7. The kidneys," *ISBN*, pp. 58528–180, 2009.

[23] Mineralogy database, webmineral.com.

[24] W. M. M. Heijnen and F. B. Van Duijneveldt, "The theoretical growth morphology of calcium oxalate dihydrate," *Journal of Crystal Growth*, vol. 67, no. 2, pp. 324–336, 1984.

[25] H. Heyer, "Kinetics of Precipitation. A. E. Nielsen. International Series of Monographs on Analytical Chemistry. Haupt-Herausg.R. Belcher undL. Gordon. Vol. 18. Pergamon Press, Oxford-London-Edinburgh-New York-Paris-Frankfurt 1964. 1. Aufl., X, 153 S., zahlr. Abb., mehrere Tab., geb. £ 2.0.0," *Angewandte Chemie*, vol. 77, no. 16, p. 745, 1965.

[26] P. Bennema and O. Söhnel, "Interfacial surface tension for crystallization and precipitation from aqueous solutions," *Journal of Crystal Growth*, vol. 102, no. 3, pp. 547–556, 1990.

[27] D. J. Kok and S. R. Khan, "Calcium oxalate nephrolithiasis, a free or fixed particle disease," *Kidney International*, vol. 46, no. 3, pp. 847–854, 1994.

[28] PG. Werness, SC. Duckworth, and LH. Smith, "Calcium oxalate dihydrate crystal growth," *Invest Urol*, vol. 17, no. 3, pp. 230–233, 1979.

[29] B. Toma□ic and G. Nancollas, "Crystal growth of calcium oxalate hydrates: A comparative kinetics study," *Journal of Colloid and Interface Science*, vol. 75, no. 1, pp. 149–160, 1980.

[30] AE. Nielsen, "Theory of electrolyte crystal growth," *ISBN*, pp. 35–44, 1981.

[31] B. Finlayson, "Pathologic mineralization, nucleation, growth and retention," *Biological Mineralization and Demineralization*, pp. 271–285, 1982.

[32] S. Somrani, M. Banu, M. Jemal, and C. Rey, "Physico-chemical and thermochemical studies of the hydrolytic conversion of amorphous tricalcium phosphate into apatite," *Journal of Solid State Chemistry*, vol. 178, no. 5, pp. 1337–1348, 2005.

[33] A. Oyane, K. Onuma, T. Kokubo, and A. Ito, "Clustering of Calcium Phosphate in the System $CaCl_2$-H_3PO_4-KCl-H_2O," *Journal of Physical Chemistry B*, vol. 103, no. 39, pp. 8230–8235, 1999.

[34] A. Dey, P. H. H. Bomans, F. A. Müller et al., "The role of prenucleation clusters in surface-induced calcium phosphate crystallization," *Nature Materials*, vol. 9, no. 12, pp. 1010–1014, 2010.

[35] L. Wang, S. Li, E. Ruiz-Agudo, C. V. Putnis, and A. Putnis, "Posner's cluster revisited: Direct imaging of nucleation and growth of nanoscale calcium phosphate clusters at the calcite-water interface," *Cryst Eng Comm*, vol. 14, no. 19, pp. 6252–6256, 2012.

[36] K. Onuma and A. Ito, "Cluster Growth Model for Hydroxyapatite," *Chemistry of Materials*, vol. 10, no. 11, pp. 3346–3351, 1998.

[37] E. Fürth, *Investigation on the theory of the Brownian movement*, Dover Publications Inc, New York, 1956.

[38] S. Stoll and S. Diez, "Fractal Structures and Mechanisms in Coagulation/Flocculation Processes in Environmental Systems: Theoretical Aspects," *Biophysical Chemistry of Fractal Structures and Processes in Environmental Systems*, vol. 11, pp. 111–148, 2008.